Mutations in Synaptojanin Disrupt Synaptic Vesicle Recycling

Todd W. Harris,* Erika Hartwieg,‡ H. Robert Horvitz,‡ and Erik M. Jorgensen*

*Department of Biology, University of Utah, Salt Lake City, Utah 84112-0840; and ‡Department of Biology, Massachussetts Institute of Technology, Cambridge, Massachusetts 02139

Abstract. Synaptojanin is a polyphosphoinositide phosphatase that is found at synapses and binds to proteins implicated in endocytosis. For these reasons, it has been proposed that synaptojanin is involved in the recycling of synaptic vesicles. Here, we demonstrate that the *unc-26* gene encodes the *Caenorhabditis elegans* ortholog of synaptojanin. *unc-26* mutants exhibit defects in vesicle trafficking in several tissues, but most defects are found at synaptic termini. Specifically, we observed defects in the budding of synaptic vesicles from the plasma membrane, in the uncoating of vesicles after fission, in the recovery of vesicles from endosomes, and in the tethering of vesicles to the cytoskeleton. Thus, these results confirm studies of the mouse synaptojanin 1 mutants, which exhibit defects in the uncoating of synaptic vesicles (Cremona, O., G. Di Paolo, M.R. Wenk, A. Luthi, W.T. Kim, K. Takei, L. Daniell, Y. Nemoto, S.B. Shears, R.A. Flavell, D.A. McCormick, and P. De Camilli. 1999. *Cell*. 99:179–188), and further demonstrate that synaptojanin facilitates multiple steps of synaptic vesicle recycling.

Key words: *Caenorhabditis elegans* • synaptic transmission • endocytosis • *unc-26* • polyphosphoinositide phosphatase

Introduction

Depolarization of neurons causes synaptic vesicles to fuse with the plasma membrane and to release their cargo of neurotransmitter into the synaptic cleft. During periods of high neuronal activity, synaptic vesicles must fuse with the plasma membrane at high rates. Sustained rates of vesicle fusion in turn are facilitated by an efficient mechanism of synaptic vesicle recycling (De Camilli and Takei, 1996). The recycling pathway recovers vesicle membrane and proteins from the plasma membrane, and returns them to the reserve pool of synaptic vesicles for subsequent rounds of release.

Synaptic vesicle recovery from the plasma membrane can be divided into four steps: clathrin coat assembly, budding, fission, and uncoating (Cremona and De Camilli, 1997). During the initial step, synaptic vesicle proteins are assembled together in the plasma membrane and marked for recycling (Miller and Heuser, 1984; Jorgensen et al., 1995; Nonet et al., 1999). The process is likely to be mediated by the clathrin adaptor complex, which subsequently recruits clathrin to the area of membrane to be recycled. In the budding step, clathrin assembles into a curved array and the membrane invaginates. In the fission step, dynamin monomers assemble into a collar around the neck of the vesicle and sever the vesicle from the plasma membrane. In the uncoating step, the clathrin and clathrin adaptor protein coat is disassembled. Vesicle uncoating must occur before vesicles can fuse to other membranes.

The phosphoinositide (PI)[1] phosphatase synaptojanin has been proposed to function within the synaptic vesicle recycling pathway. Synaptojanin is defined by three domains (McPherson et al., 1994, 1996): a polyphosphoinositide phosphatase domain similar to the yeast Sac1 protein (Chung et al., 1997; Guo et al., 1999), a PI 5–phosphatase domain, and a proline-rich domain. Three attributes of synaptojanin suggest a role in synaptic vesicle recycling: its location, its protein interactions, and its lipid substrate specificity.

First, the location of synaptojanin is consistent with a role for the protein in the endocytosis of synaptic vesicles. Synaptojanin is highly enriched in the brain and is located at nerve terminals, and it is associated with synaptic vesicles and coated endocytic intermediates (McPherson et al., 1994; Haffner et al., 1997). Moreover, the distribution of synaptojanin is coincident with that of other endocytic

Address correspondence to Erik M. Jorgensen, Department of Biology, University of Utah, 257 South 1400 East, Salt Lake City, UT 84112-0840. Tel.: 801 585-3517. Fax: 801 581-4668. E-mail: jorgensen@biology.utah.edu

[1]*Abbreviations used in this paper:* Ce-synaptojanin, *Caenorhabditis elegans* synaptojanin; EST, expressed sequence tag; GABA, γ-aminobutyric acid; GFP, green fluorescent protein; ORF, open reading frame; PI, phosphoinositide.

proteins, such as amphiphysin and dynamin (McPherson et al., 1994, 1996).

Second, synaptojanin binds a complex of proteins implicated in endocytosis. Synaptojanin binds to amphiphysin and endophilin directly (McPherson et al., 1996; Micheva et al., 1997). Amphiphysin also binds to both the GTPase dynamin and the α subunit of the AP2 clathrin adaptor complex (David et al., 1996; Grabs et al., 1997). Moreover, synaptojanin, dynamin, and amphiphysin can be isolated in a complex with the clathrin adaptor AP2. A similar complex can be isolated lacking amphiphysin, but including endophilin (Micheva et al., 1997; Slepnev et al., 1998). Injection of the SH3 domains of amphiphysin (into lamprey terminals) or of endophilin (into a reconstituted in vitro assay) blocks endocytosis via a dominant-negative disruption of protein interactions central to the complex (Shupliakov et al., 1997; Wigge et al., 1997; Simpson et al., 1999), illustrating the importance of these complexes in synaptic vesicle recycling.

Third, proteins implicated in endocytosis have been shown to bind to the lipid substrates of synaptojanin. Synaptojanin is a polyphosphoinositide phosphatase, capable of selectively cleaving the 3-, 4-, and 5-phosphates from PI(3)P, PI(4)P, PI(3,5)P_2, PI(4,5)P_2, and PI(3,4,5)P_3 (McPherson et al., 1996; Chung et al., 1997; Woscholski et al., 1997; Guo et al., 1999). The Sac1 domain of synaptojanin acts as a 3-, 4-, and 5-polyphosphoinositide phosphatase; at least in yeast, the PI 4-phosphatase activity of this domain appears to be the most prominent (Guo et al., 1999). The second phosphatase domain provides PI 5-phosphatase activity. These dual phosphatase domains, encoded within a single polypeptide chain, are reflected in the protein's namesake, Janus, the two-faced Roman god of gateways. Since a number of proteins of the core endocytic complex bind to PI(4,5)P_2, including dynamin, synaptotagmin, AP2, and AP180, the phosphatase activity of synaptojanin may regulate the recruitment of endocytic proteins to the plasma membrane (De Camilli et al., 1996; Schiavo et al., 1996; Zheng et al., 1996; Hao et al., 1997; Jost et al., 1998; Gaidarov and Keen, 1999).

The phenotype of synaptojanin 1 mutant mice supports a role for synaptojanin in the uncoating step of the recycling pathway (Cremona et al., 1999). Deletion mutations of the synaptojanin gene lead to 100% lethality within 15 d of birth. These animals exhibit an accumulation of clathrin-coated vesicles at nerve terminals in both the whole animal and in cultured cortical neurons. In vitro studies on protein-free liposomes derived from mutant or wild-type animals show increased formation of clathrin-coated structures in the mutant. These observations indicate a role for synaptojanin in the uncoating of vesicles, but do not reveal a role for PIs in earlier steps in the recycling pathway, such as clathrin recruitment or vesicle fission.

We cloned and characterized the synaptojanin ortholog of *Caenorhabditis elegans*, and showed that it is encoded by the *unc-26* gene. *unc-26* mutants exhibit a depletion of vesicles at synapses, an accumulation of endocytic pits, and an accumulation of coated vesicles. These defects are consistent with a role for synaptojanin at several steps in the endocytosis of synaptic vesicles. In addition, *unc-26* mutants have cytoskeletal abnormalities and vesicle trafficking defects, suggesting broader roles for synaptojanin and PI lipids in maintenance of the cytoskeleton and in vesicle trafficking.

Materials and Methods

Strains and Alleles

Strains used in this study were maintained using standard techniques (Brenner, 1974). The wild type was N2 Bristol. The following mutations were used in this study: LG IV, *unc-26: e205, e314, e345, e429, e446, e568, e1048, e1196, m2, n1307, n1308n1307, ox1, s1710*; *unc-22(s7); dpy-4(e1166sd)*. Most strains are available from the *C. elegans* Genetics Center.

Molecular Characterization of C. elegans Synaptojanin

A BLASTP Genbank database search using full-length rat synaptojanin revealed four *C. elegans* expressed sequence tags (ESTs): yk32c3, yk27c9, yk3c11, and yk16a11, belonging to the overlapping EST group CELK00306. Primers were designed against the sequence of the ESTs and used to amplify a 2-kb genomic region from wild-type DNA. This fragment was used to probe 70,000 plaques from a phage *C. elegans* genomic DNA library. We isolated three genomic clones that extended ~5 kb past the end of cosmid JC8. A 10-kb HindIII fragment extending into the gap was subcloned from one of these clones, and the sequence of the nonoverlapping region was determined. None of these clones contained the complete 5′ end of the open reading frame (ORF).

To obtain the 5′ sequence of the gene, we first screened a cDNA library using the 2-kb genomic fragment. We isolated a single cDNA from this screen, UNC-26C. 5′ splice leader rapid amplification of cDNA ends (RACE)-PCR enabled us to clone the remaining 5′ end of the cDNA. Both SL1 and SL2 splice transcripts were isolated. The remaining 3′ sequence was obtained by determining the restriction pattern of the initial four ESTs and then defining the sequence of the longest cDNA clone, yk32c3.

To demonstrate that *unc-26* encodes Ce-synaptojanin, Southern blots of total worm genomic DNA from *unc-26(n1307)*, and the revertant allele *unc-26(n1308n1307)* were probed with the initial 2-kb synaptojanin genomic fragment. This analysis revealed a restriction polymorphism in *unc-26(n1307)* that is restored to wild-type size in the revertant allele. The sequence of this region of *unc-26(n1307)* was sequenced and found to contain a tandem duplication of ~650 bp within the first intron of the gene. We determined the sequence of 12 additional *unc-26* alleles, using intragenic mapping as a guide for sequence determination (Charest et al., 1990). Approximately 20 homozygous mutant worms were placed in lysis buffer (50 mM KCl, 10 mM Tris, pH 8.2, 2.5 mM $MgCl_2$, 0.45% NP-40, 0.45% Tween-20, 0.01% gelatin, 1 mg/mL proteinase K), incubated for 1 h at 65°C, followed by 15 min at 95°C. A series of primer sets were used to amplify the corresponding genomic region, and sequences of the PCR products were determined using the Thermosequenase cycle sequencing system (Amersham Pharmacia Biotech) or an ABI automated sequencer.

Mutant Analysis

Strength of Alleles. *unc-26* alleles were scored for their relative degree of mobility as larva and adults, growth rate, and overall body shape and size.

Nervous System Architecture. *unc-26(s1710)* was crossed into strains containing integrated arrays expressing green fluorescent protein (GFP) under the control of the *unc-47* promoter [EG1285: *lin-15(n765ts) oxIs12(P_{unc-47}:GFP)*] or expressing synaptobrevin-GFP (SNB-GFP) under the control of the *unc-25* promoter [MT8247: *lin-15(n765ts) nIs52(P_{unc-25}:SNB-GFP)*]. The resulting strains were analyzed using confocal microscopy. Relative levels of synaptobrevin-GFP fluorescence at the cell body were determined in blind studies. 10 wild-type animals or 10 *unc-26(s1710)* animals were placed on a single microscope slide, and scored as wild-type or mutant based on cell body fluorescence. In 10 of 10 tests, all slides were scored correctly as either mutant or wild-type.

Ultrastructural Analysis. BC3213 *unc-22(s7) unc-26(s1710) dpy-4(e1166sd)* was outcrossed against the wild type. Both arms of chromosome IV were outcrossed by removing flanking markers resulting in the strain EG1349 *unc-26(s1710)*. EG1349 *unc-26(s1710)* was fixed for EM as previously described (Jorgensen et al., 1995). 433 ultrathin (~33 nm) serial sections were cut from four different worms. Images were recorded at 15,000-, 20,000-, or 25,000×. The ventral nerve cords were reconstructed from prints and the relevant structures were quantified in all sets. These

data were compared with reconstructions of wild-type ventral nerve cords (328 sections) derived from two worms.

Vesicle Depletion. The average number of synaptic vesicles per synapse was determined in the cholinergic neurons VA and VB, and in the γ-aminobutyric acid (GABA) neuron VD. These neurons were identified by their dorsal/ventral positioning within the ventral nerve cord, and by their polarization: VA and VB neurons synapse on other neurons and muscle, whereas VD is directed solely to muscle (White et al., 1976). Synapses were defined to be any axon profile containing a morphologically defined electron-dense presynaptic specialization, including lateral sections until the number of synaptic vesicles in the profile dropped below the total average number of synaptic vesicles in all sections (wild-type = 9 synaptic vesicles; *unc-26(s1710)* = 5 synaptic vesicles), and no fewer than two lateral sections on each side.

Endocytic Pits and Coated Vesicles. The presence of endocytic pits in VA, VB, and VD neurons was quantified. To avoid counting ripples in the membrane as endocytic pits, we scored invaginations as an endocytic pit only if they were present in a single section and did not continue into lateral sections. The distribution of these pits relative to active zones was quantified by measuring their distance to the nearest active zone in sections, where each section represents 33 nm. Pits found within sections containing an active zone were pooled into the <33-nm distance bin. The average number of pits at this distance was calculated by dividing the number of pits by the total number of sections at this distance. The average number of pits at any given distance in lateral sections was calculated by dividing the number of pits scored by twice the number of sections at that distance, to account for the double representation of each distance on either side of the synapse. Coated vesicles were scored and their distribution quantified using the same methodology as that outlined for endocytic structures.

Endosomal Compartments. The presence of recognizable endosomal structures in VA, VB, and VD neurons was noted. An endosomal structure was defined as an amorphous vesicle >50 nm that extended two or more lateral sections.

Results

Cloning of C. elegans Synaptojanin

C. elegans synaptojanin (Ce-synaptojanin) was cloned using a homology-based approach. BLAST searches using the rat synaptojanin sequence revealed a set of overlapping ESTs encoding predicted proteins highly similar to the vertebrate protein. This EST group hybridized to YAC Y67H2 on linkage group IV. However, only a small 3′ portion of the consensus sequence was contained on cosmids covered by the YAC, indicating that most of the synaptojanin gene resided within the cosmid gap between cosmids JC8 and W02A2 (Fig. 1 A). We isolated phage clones that extended into the gap, but these clones lacked the 5′ end of the gene. The remaining 5′ end of the ORF was determined by sequencing full-length cDNAs. The sequence of the 5′ end of the cDNA was used to amplify the genomic DNA from which the complete gene sequence was determined.

An analysis of the cDNAs revealed that the locus is a nematode ortholog of synaptojanin. The longest predicted Ce-synaptojanin protein is 1,119 amino acids and contains the three defining domains of synaptojanin: an amino-terminal Sac1-like polyphosphoinositide phosphatase domain, a PI 5-phosphatase domain, and a COOH-terminal proline-rich domain (Fig. 2). The predicted protein is 43% identical to the rat protein, showing the highest degree of identity in the Sac1 (46%) and 5-phosphatase (43%) domains. Although there are four predicted inositol 5-phosphatases and at least four Sac1 domain-containing proteins encoded in the *C. elegans* genome (data not shown), Ce-synaptojanin is the only predicted ORF containing the three canonical domains of synaptojanin.

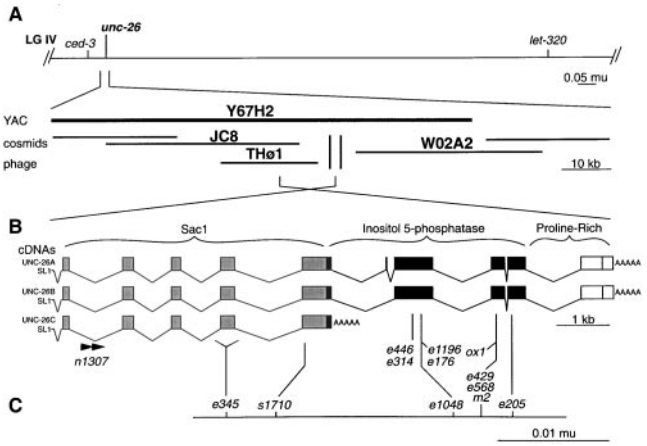

Figure 1. Characterization of the Ce-synaptojanin locus. A, Genetic and physical maps. *unc-26* maps to linkage group IV, between *ced-3* and *let-320*. Below the genetic map is a representation of the physical map of this region, showing YACs, cosmids, and phage clones. A cosmid gap (vertical lines) existed in this region. Phage clones (THø1) extended from the end of JC8, but did not contain the complete ORF. B, Predicted mRNAs. UNC-26A (2/12 cDNAs). UNC-26B (9/12 cDNAs). UNC-26C (1/12 cDNAs). The 5′ end of UNC-26C was incomplete, and its 5′ splice pattern of exons was inferred from the other variants. This variant was generated by readthrough of the splice junction at the end of exon 5. UNC-26A and B splice variants generate transcripts with 3 nt of 5′ untranslated sequence and 311 nt of 3′ untranslated sequence. The UNC-26C variant generates a transcript with 21 bp of 3′ untranslated sequence. C, *unc-26* mutations were mapped relative to each other (Charest et al., 1990). The order and position of sequenced mutations corresponded to their genetic map positions. *e176*, *e314*, *e446*, *e1196*, *n1307*, and *ox1* were not mapped relative to other alleles and are indicated only for reference.

Ce-synaptojanin cDNAs defined three splice variants. 2 of 12 cDNAs represented the longest isoform and this splice variant most closely resembles the vertebrate protein (Fig. 1 B, UNC-26A). UNC-26A differs from the most abundant variant (Fig. 1 B, UNC-26B, 9 of 12 cDNAs) only by the presence of a single exon insertion encoding six amino acids within the phosphatase domain (Fig. 2). Finally, a single cDNA was isolated that encodes a truncated protein, containing only the Sac1 domain, and lacking the phosphatase and proline-rich domains (Fig. 1 B, UNC-26C). Conversely, in vertebrates, splice variants lacking the Sac1 domain, but retaining the 5-phosphatase and proline-rich domains have been identified. These variants retain full 5-phosphatase activity (Woscholski et al., 1998). In yeast, Sac1 domain-containing proteins are expressed alone from the SAC1 gene or together with a 5-phosphatase domain in the INP5 gene products (Guo et al., 1999). These observations suggest that the Sac1 and 5-phosphatase domains possess distinct and separable functions.

We demonstrated that synaptojanin is encoded by the *unc-26* gene by analyzing mutations of the locus. Because *unc-26* genetically maps within a 0.67-map unit interval spanning the physical region containing Ce-synaptojanin (Fig. 1 A), it was a strong candidate gene for this ORF. We

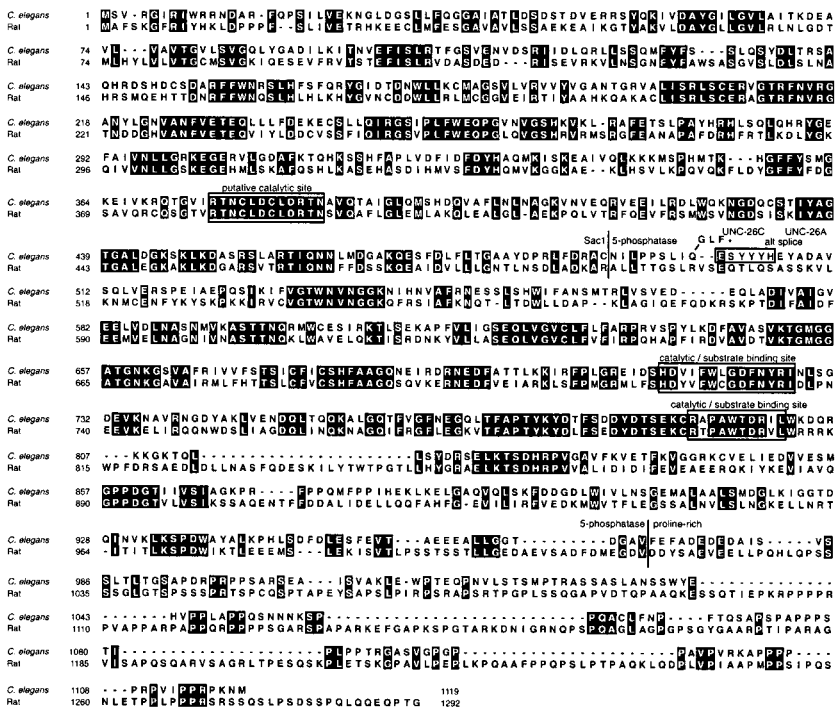

Figure 2. Ce-synaptojanin (Genbank/EMBL/DDBJ accession numbers for UNC-26A, B, and C are AF283322, AF283323, and AF283324, respectively) aligned with rat synaptojanin (Genbank/EMBL/DDBJ accession number U45479). Identities are in black boxes. The single exon difference between the splice variants UNC-26A and B is boxed, and the alternative coding residues and truncation of the UNC-26C transcript is shown above where it diverges from the other splice forms. Also indicated are the putative catalytic site for Sac1-like phosphatases (Guo et al., 1999) and the highly conserved catalytic and/or substrate binding regions of 5-phosphatases (Communi and Erneux, 1996; Communi et al., 1996; Jefferson and Majerus, 1996; Stolz et al., 1998).

determined the sequences of the synaptojanin gene from 13 *unc-26* alleles, and all 13 alleles contained mutations in this ORF (Table I). The linear order of the *unc-26* mutations within the gene corresponds to their previously determined (Charest et al., 1990) intragenic map positions (Fig. 1 C), demonstrating that *unc-26* encodes Ce-synaptojanin. Further proof is provided by an unstable allele; the duplication associated with the *unc-26(n1307)* allele is restored to both wild-type size on genomic Southern blots and wild-type sequence in the revertant allele *unc-26(n1308n1307)* (data not shown). The best candidate for a null allele is *unc-26(s1710)*, a five-nucleotide deletion that results in a protein truncated within the NH_2-terminal Sac1 domain.

Neurotransmission Defects

Behavioral and pharmacological analyses indicate that *unc-26* mutants possess a presynaptic disruption of cholinergic and GABA neurotransmission. First, *unc-26* mutants resemble mutants lacking the biosynthetic enzyme for acetylcholine encoded by the *cha-1* gene. Mutations in *cha-1* (and *unc-26*) result in characteristic locomotory defects: animals are small, move backwards with a jerky motion,

Table I. Sequence of unc-26 Alleles

Allele	Mutagen	DNA change		Amino acid change	Domain	Phenotypic strength
		Wild-type	Mutant			
e176	EMS	Gat	Aat	D722N	Phosphatase	Strong
e205	EMS	tGg	tAg	W903stop	Phosphatase	Strong
e314	EMS	gGa	gAa	G662E	Phosphatase	Weak
e345	Spontaneous	415-bp deletion		In-frame deletion of aa183-280	Sac1	Strong
e429	EMS	Gat	Aat	D825N	Phosphatase	Weak
e446 (1st site)	EMS	Gag	Tag	E623stop	Phosphatase	Strong
e446 (2nd site)	EMS	aGa	aCa	R709T	Phosphatase	Strong
e568	EMS	Cga	Tga	R799stop	Phosphatase	Moderate
e1048sd	EMS	Gga	Aga	G721R	Phosphatase	Strong
e1196	ICR	gat	gGa	Frameshift at 732, stop at 733	Phosphatase	Strong
m2	ICR	tgG	tgA	W796stop	Phosphatase	Strong
n1307	Spontaneous	~650-bp tandem duplication in 1st intron		–	Sac1	Strong
ox1	EMS	tgG	tgA	W802stop	Phosphatase	Strong
s1710	*mut-4* mutator	gAT GCG ttc	gtt caa aac	Frameshift at 309, stop at 328	Sac1	Strong

and frequently coil (Rand and Russell, 1984; Alfonso et al., 1994). Second, *unc-26* mutants are strongly resistant to inhibitors of acetylcholinesterase, indicative of a decrease in acetylcholine release (Rand and Russell, 1985; Nguyen et al., 1995; Miller et al., 1996; Yook, C., and E.M. Jorgensen, personal communication). Third, *unc-26* mutants display abnormalities associated with the loss of GABA neurotransmission. For example, mutations that eliminate GABA synthesis disrupt the enteric muscle contractions of the defecation cycle (McIntire et al., 1993; Jin et al., 1999) and *unc-26* mutants have reduced numbers of enteric muscle contractions (Miller et al., 1996). Taken together, these data indicate defects in both cholinergic and GABA function in *unc-26* mutants.

Although these abnormalities suggest a defect in synaptic function, they could also arise through defects in development of the nervous system. We examined the architecture of the GABA nervous system in *unc-26* mutants using an *unc-47*-GFP reporter construct that expresses GFP in all 26 GABA neurons (McIntire et al., 1997). In the null allele *unc-26(s1710)*, all 26 cell bodies were properly positioned and the axonal architecture appeared normal (wild-type, $n = 4$ animals; *unc-26(s1710)*, $n = 5$ animals; data not shown). These results suggest that the nervous system develops normally, and that the locomotory defects are likely to be caused by aberrant function of the nervous system, possibly by defects in the endocytosis of synaptic vesicles.

Synaptic Vesicle Distribution Defects

To determine if there were defects in the recycling of synaptic vesicles in *unc-26* mutants, we reconstructed serial electron micrographs of the ventral nerve cord of wild-type and *unc-26(s1710)* animals. *unc-26(s1710)* animals exhibited two defects in the distribution of synaptic vesicles at synapses. First, the total number of synaptic vesicles at synapses was depleted relative to the wild type. Second, the remaining vesicles exhibited linear arrangements and were dissociated from the active zone.

Qualitatively, *unc-26* mutants exhibited a depletion of vesicles at synapses relative to the wild type (Fig. 3 A). Quantification of vesicles at synapses in the cholinergic and GABA-releasing motor neurons demonstrated that the number of vesicles per synapse in *unc-26(s1710)* animals (74 ± 4.8 vesicles/synapse, $n = 85$ synapses) was reduced to 38% of the number of synaptic vesicles in the wild type (194 ± 19.6 vesicles/synapse, $n = 46$ synapses; Fig. 3 B). This decrease suggested that *unc-26* mutants are defective in synaptic vesicle endocytosis, or alternatively, in the transport of vesicles from the cell body (Jorgensen et al., 1995).

To test for defects in vesicle transport from the cell body, we looked for the presence of vesicles in motor neuron cell bodies in the null mutant *unc-26(s1710)*. At the ultrastructural level, 10 of 24 mutant cell bodies examined exhibited an accumulation of vesicles (Fig. 4 A); no accumulation was observed in the wild type (11 cell bodies examined). Although some cell bodies exhibited an accumulation of vesicles, it was unclear if these vesicles were synaptic vesicle precursors or Golgi complex trafficking intermediates. To distinguish between these possibilities, we determined if synaptic vesicle proteins were transported

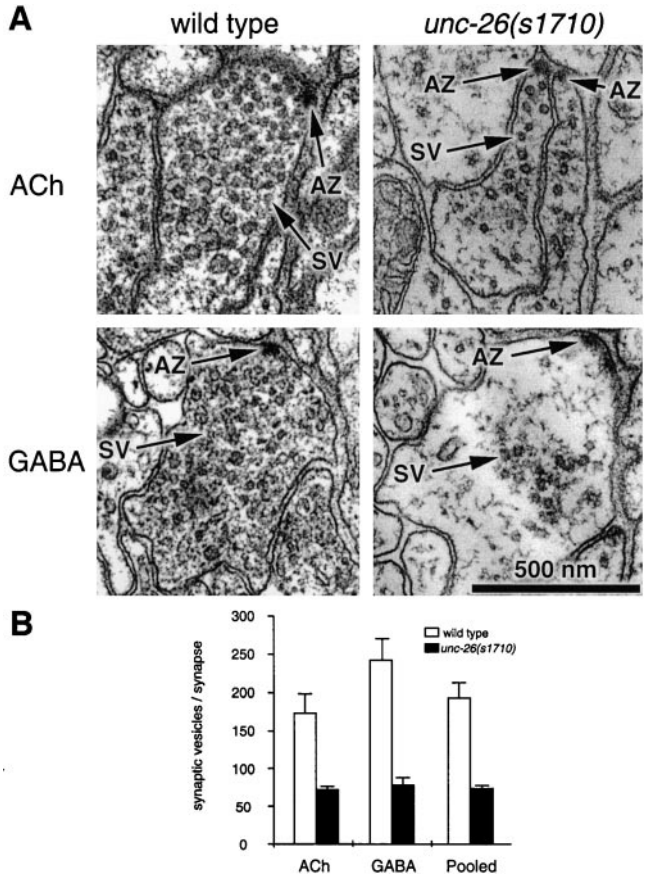

Figure 3. Mutations in the *unc-26* gene cause a depletion of synaptic vesicles at neuromuscular synapses. A, Representative electron micrographs of acetylcholine and GABA neuromuscular junctions in a wild-type (left) and an *unc-26(s1710)* adult hermaphrodite (right). The ventral nerve cord was reconstructed from serial electron micrographs. GABA neurons were identified based on their position within the cord, and because they form synaptic connections exclusively to muscle. Cholinergic neurons were identified based on their position in the cord and because they form synaptic connections to neurons and muscle (White et al., 1976). SV, Synaptic vesicle; AZ, active zone. B, The average number of synaptic vesicles per reconstructed synapse was decreased in *unc-26* mutants. Number SV per synapse: ACh, wild-type = 173 ± 25 SV, $n = 32$ synapses; *unc-26(s1710)* = 72 ± 5 SV, $n = 61$ synapses. GABA, wild-type = 242 ± 28 SV, $n = 14$ synapses; *unc-26(s1710)* = 78 ± 10 SV, $n = 23$ synapses. Pooled, wild-type = 194 ± 19 SV, $n = 46$ synapses; *unc-26(s1710)* = 74 ± 4 SV, $n = 85$ synapses.

to sites of release. Specifically, we examined the distribution of the synaptic vesicle protein synaptobrevin in *unc-26(s1710)* animals. Wild-type worms expressing synaptobrevin tagged with GFP exhibited punctate staining along the ventral and dorsal nerve cords. These puncta correspond to pools of vesicles at synapses (Jorgensen et al., 1995; Nonet, 1999). In *unc-26* mutants, a similar level of synaptobrevin-GFP fluorescence was observed at synapses along the nerve cords (Fig. 4, B and C), indicating that most synaptic vesicle precursors are appropriately delivered to synapses. In blind tests, we detected a slight increase in the fluorescence of some, but not all, motor neu-

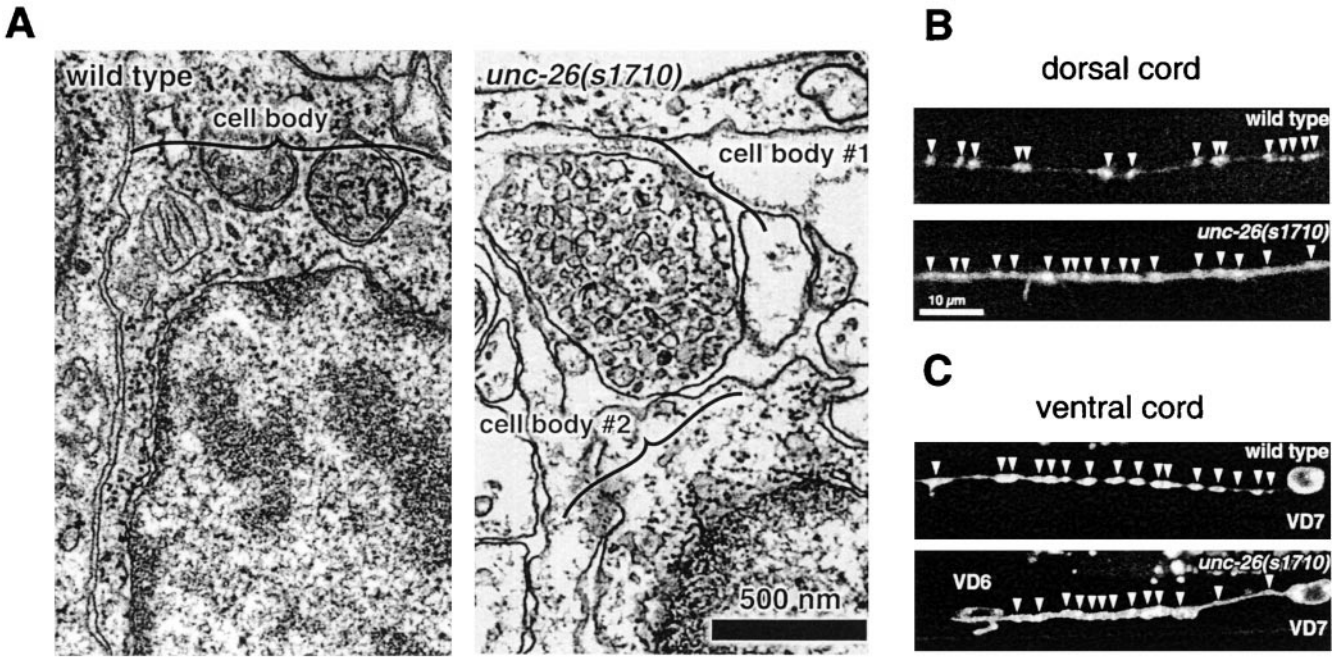

Figure 4. Vesicle transport was partially disrupted in *unc-26*. A, left, Electron micrograph of a motor neuron cell body from a wild-type adult hermaphrodite. Right, Motor neuron cell bodies in an *unc-26(s1710)* adult hermaphrodite. Note large accumulation of vesicles at cell body #1, but absence of vesicles in cell body #2. 10 of 24 cell bodies examined in the mutant exhibited this congestion of vesicles, whereas 0 of 11 wild-type cell bodies exhibited this accumulation. B, Synaptobrevin-GFP distribution in the dorsal nerve cord of wild-type and *unc-26* adult hermaphrodites. Synaptobrevin-GFP was localized to synaptic varicosities (arrowheads) in the wild type and in *unc-26(s1710)* animals. However, synaptobrevin-GFP was more diffuse at synapses in *unc-26(s1710)*, rather than punctate as in the wild type. C, Synaptobrevin-GFP distribution in the ventral nerve cord of wild-type and *unc-26(s1710)* adult hermaphrodites. Synaptic varicosities (arrowheads) along the ventral nerve cord exhibited the same diffuse staining pattern as seen along the dorsal cord.

ron cell bodies (see Materials and Methods). These data suggest that in some cells, synaptic vesicle precursors are not transported as efficiently in the synaptojanin mutant. However, in most cells, transport of synaptic vesicle proteins was normal, therefore the depletion of synaptic vesicles at the synapse was likely to be caused by a defect in endocytosis.

Endocytosis Defects

To ascertain whether there was a defect in the recovery of synaptic vesicle components from the plasma membrane, we further characterized the distribution of synaptobrevin-GFP in *unc-26(s1710)* mutants. In wild-type animals, fusion of synaptic vesicles at the active zone delivers synaptobrevin to the plasma membrane. Synaptobrevin is recovered from the membrane by endocytosis and regenerated synaptic vesicles are clustered at the active zone, preserving a punctate staining of synaptic varicosities (Fig. 4, B and C). In mutants that have defects in synaptic vesicle endocytosis, such as in synaptotagmin and AP180 mutants, synaptobrevin-GFP is diffusely distributed in the plasma membrane of axons (Jorgensen et al., 1995; Nonet et al., 1999). *unc-26* mutants exhibited a similarly diffuse staining pattern of synaptobrevin-GFP along the nerve cords (Fig. 4, B and C), indicating that at least this synaptic vesicle protein is not efficiently recovered from the plasma membrane, and suggesting that synaptic vesicle membrane remains in the plasma membrane longer in *unc-26* mutants.

Our ultrastructural analysis of neuromuscular junctions confirmed that *unc-26* mutants are defective in synaptic vesicle recycling by revealing an accumulation of endocytic pits in the plasma membrane. These endocytic pits had faint collars at the neck of the budding vesicle; such collars are likely to be dynamin polymers, which are known to form rings visible by EM (Takei et al., 1995). The endocytic pits fell into two morphological classes: those coated by matrices resembling clathrin cages, and those lacking a coat (Fig. 5 A). The presence of two distinct types of endocytic pits suggests that multiple recycling pathways may exist at *C. elegans* neuromuscular junctions. Most of these pits were found within 100 nm of active zones (Fig. 5 B), and therefore, these structures are likely to be intermediates in the synaptic vesicle recycling pathway. Noncoated pits were often found immediately adjacent to active zones (Fig. 5 C). Such intermediate endocytic structures were not found at any synapses in the wild-type (wild-type, $n = 328$ sections; *unc-26(s1710)*, $n = 433$ sections). The presence of these endocytic pits indicated a vesicle membrane recycling defect in *unc-26* mutants, suggesting that the recycling pathway is slowed, allowing for the accumulation of short-lived endocytic intermediates. However, the number of these structures could not account for the depletion of mature vesicles at synapses. Thus, the loss of vesicles was likely to be due to

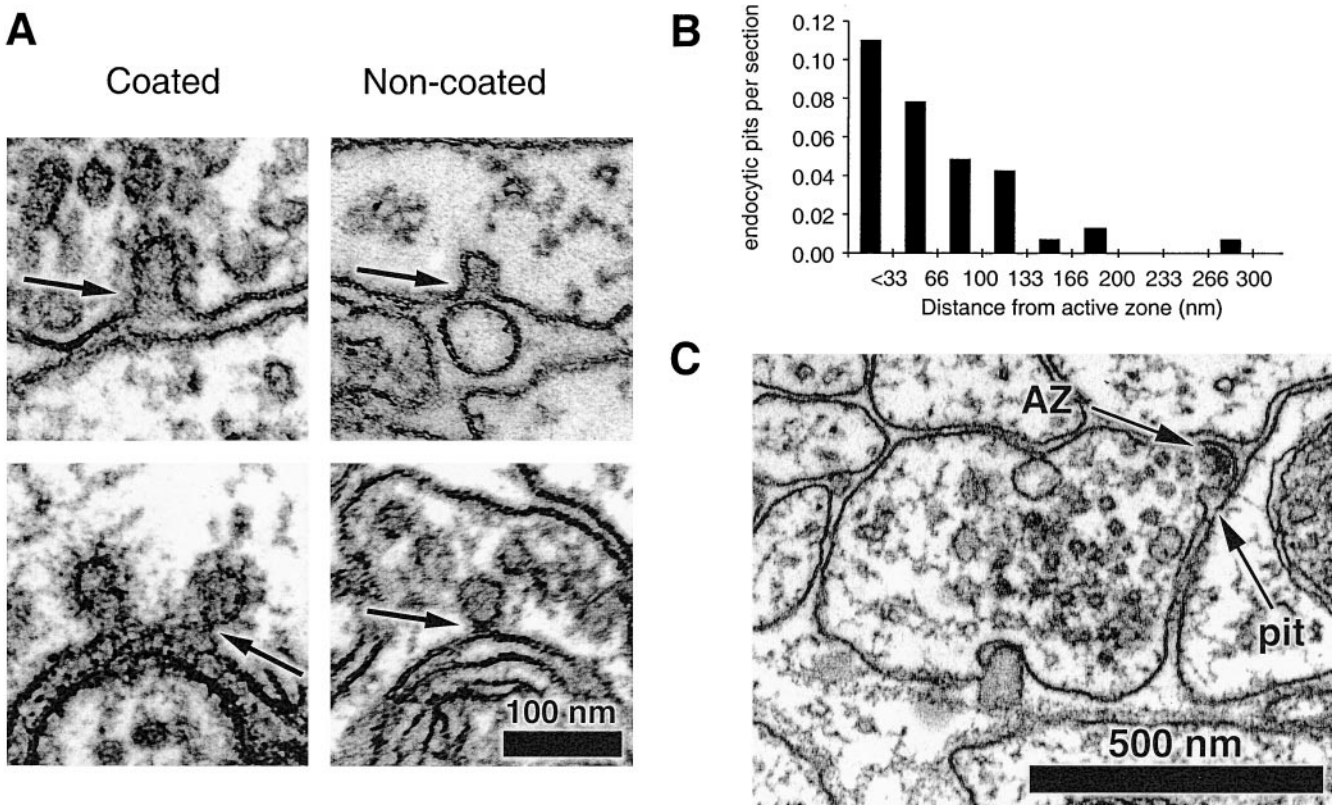

Figure 5. Endocytic pits accumulated in the plasma membrane of *unc-26(s1710)* mutants. A, Representative electron micrographs of endocytic pits from neuromuscular junctions of *unc-26(s1710)* adult hermaphrodites. Endocytic pits were either coated (left) or noncoated (right) and were observed with open necks (top) or closed necks (bottom). Pits had faint collars (arrows). No endocytic pits were observed in wild-type sections prepared using the same fixation protocol. B, Endocytic pits accumulated near electron-dense active zones in *unc-26* mutants. Plotted is the average number of pits per section at given distances from the nearest active zone (see Materials and Methods). Total number of pits scored, 58. C, Noncoated pits were often seen immediately adjacent to active zones. AZ, Active zone.

delays at a previous step, such as in clathrin recruitment or vesicle budding.

Synaptojanin mutants also accumulated coated vesicles. These vesicles were not attached to the membrane, yet still retained their clathrin coat (Figs. 6 A and 7 A). Some of these vesicles were likely to be recycling synaptic vesicles, because of their close association with synapses (Fig. 6 B). *unc-26(s1710)* animals contained an almost tenfold increase in the number of coated vesicles over the wild-type (Fig. 6 C, left). Although our serial reconstruction focused on the neuromuscular junction-rich ventral nerve cord, coated vesicles were found in a number of different cell types, but were seen predominantly in neurons, at both synapses, and in cell bodies (Fig. 6 C, right). Coated vesicles found in cell bodies were usually near Golgi stacks (Fig. 6 D). These vesicles were likely to have been trans-Golgi complex trafficking intermediates, since some could still be seen attached to Golgi stacks. The presence of coated vesicles at both the Golgi complex and the synapse in *unc-26* mutants suggest similarities between uncoating mechanisms acting on AP1 and AP2 clathrin complexes. A defect at the Golgi complex is not altogether surprising, since the synaptojanin-related INP5 proteins in yeast and the OCRL protein in animals have been implicated in Golgi complex function (Olivos-Glander et al., 1995; Suchy et al., 1995; Bensen et al., 2000). The accumulation of coated vesicles in diverse tissues indicated that, in the absence of synaptojanin, the uncoating process is blocked or delayed for synaptic vesicle endocytosis, as well as for other trafficking events.

Mutations in synaptojanin also caused an increase in endosome-like compartments (Fig. 7, A and B). Endosomes predominantly accumulated in regions with active zones; the presence of endosomes fell as distance from the active zone increased (data not shown). Because endosomes were often seen adjacent to morphologically identified active zones (Fig. 7 A), these structures may represent sorting compartments in synaptic vesicle biogenesis. These defects suggest a role for synaptojanin at the endosome analogous to its role at the plasma membrane. Alternatively, they may reflect an indirect effect of disrupted trafficking from the plasma membrane.

Cytoskeletal Defects

After synaptic vesicles are regenerated from endosomes or the plasma membrane, they must be clustered at the synapse to provide a reserve pool of vesicles for future neurotransmission events. One possible mechanism for this clustering is via interactions with the synaptic cyto-

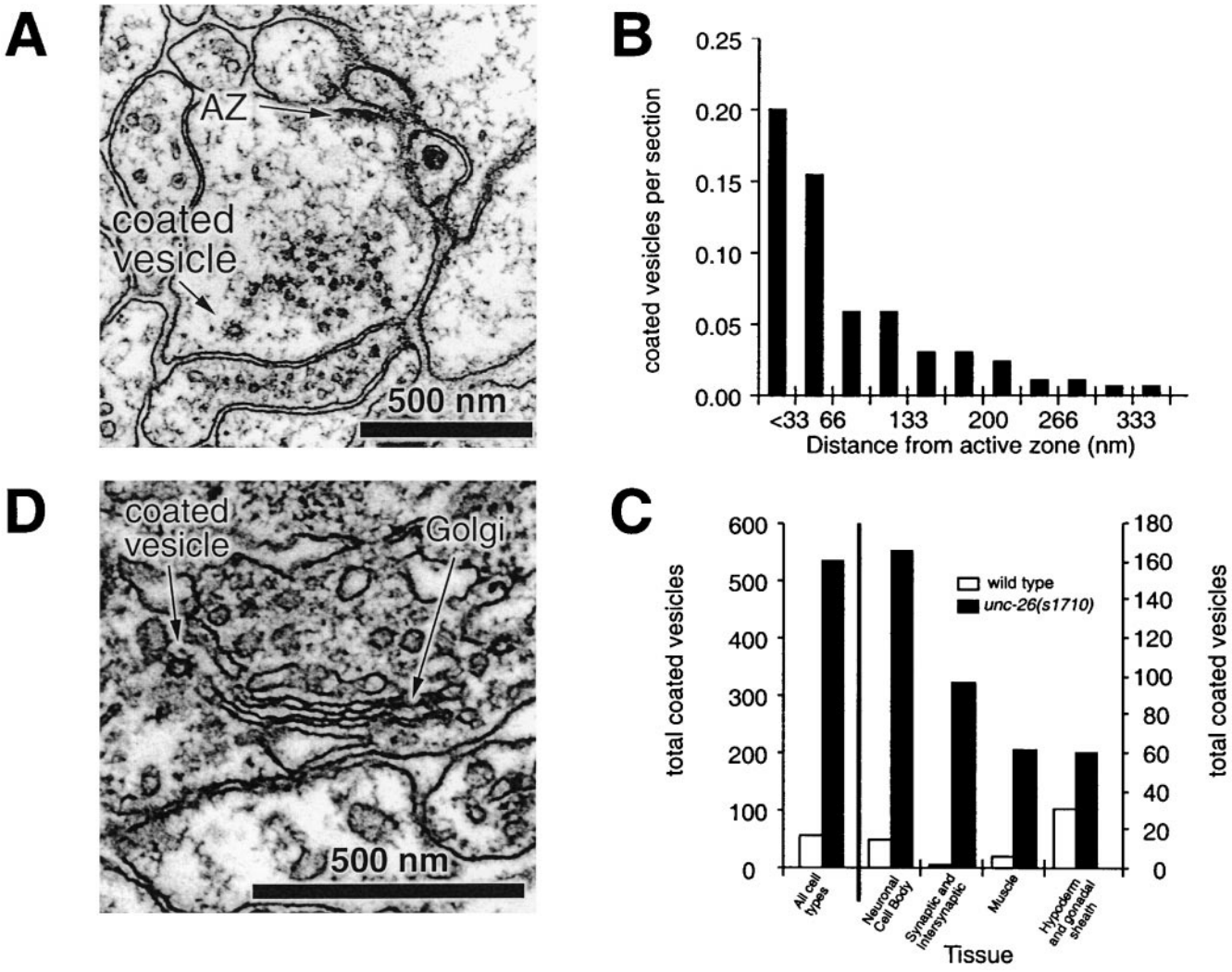

Figure 6. Coated vesicles accumulated in *unc-26* mutants. A, An example of a coated vesicle in a VD GABA motor neuron of an *unc-26(s1710)* adult hermaphrodite. AZ, Active zone. B, Coated vesicles accumulated near electron-dense active zones in *unc-26* mutants. Plotted is the average number of coated vesicles per section found in axons of *unc-26(s1710)* adult hermaphrodites at given distances from the nearest active zone. C, Quantification of coated vesicles in various tissues of wild-type and *unc-26(s1710)* adult hermaphrodites. Left, Total coated vesicles scored in muscles, hypodermis, neurons, and gonadal sheath cells in sections of the ventral nerve cord. Scale is to the left. Number of sections: wild-type, 328 sections, from two worms; *unc-26(s1710)*, 433 sections, from four worms. Right, total coated vesicles in each tissue visible in these sections. Scale is to the right. D, A coated vesicle in the cell body of a motor neuron. Such coated vesicles were often associated with Golgi stacks.

skeleton (Fernandez-Chacon and Sudhof, 1999). In *unc-26(s1710)* mutants, we observed an abnormal organization of the reserve pool, suggesting that vesicle interactions with the cytoskeleton are altered in the mutant. In the wild-type, vesicles cluster in a sphere around the active zone (Fig. 8 A). In *unc-26(s1710)* animals, fewer vesicles were seen closely associated with the active zone. Instead, most vesicles were distant from the active zone, and arranged in a linear string-of-pearls configuration (Fig. 8 B). This linear arrangement suggested that vesicles were attached along a single cytoskeletal filament or lamella. A collapse in cytoskeletal architecture in the *unc-26* mutant is consistent with observations implicating synaptojanin and PI metabolism in maintenance of the actin cytoskeleton (Sakisaka et al., 1997; Raucher et al., 2000). Surprisingly, these cytoskeletal defects did not affect the architecture of the nervous system in the adult animal (data not shown; see Materials and Methods).

Discussion

We cloned the single Ce-synaptojanin gene, and demonstrated that it corresponds to the mutationally defined gene, *unc-26*. We observed defects indicating that synaptojanin functions in general trafficking events in all tissues: coated vesicles accumulated in muscles, neurons, and the hypodermis. Moreover, noncoated vesicle trafficking intermediates accumulated to high levels in some cell bodies, suggesting defects in general vesicle trafficking. However, two observations suggested that although syn-

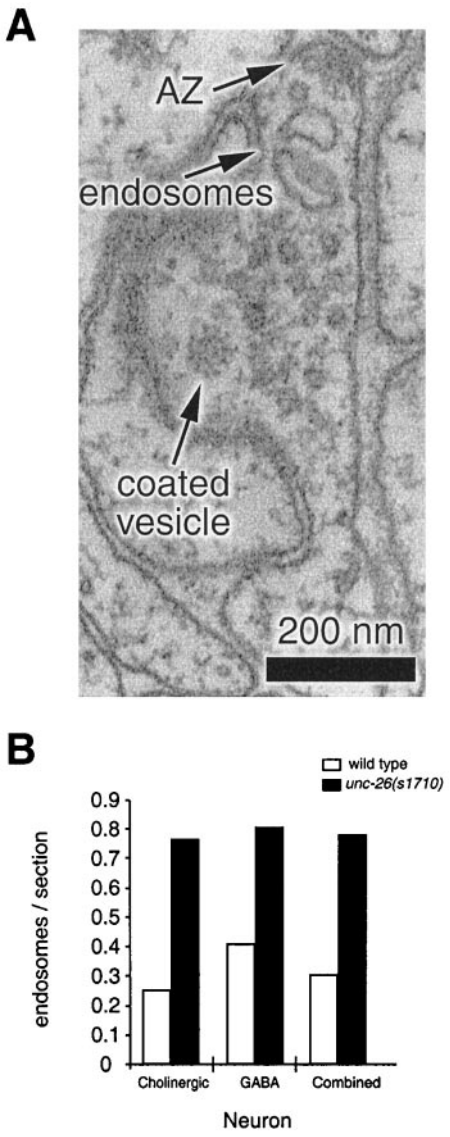

Figure 7. Endosome-like compartments accumulated in *unc-26*. A, Electron micrograph of a synapse in the VB cholinergic motor neuron of an *unc-26(s1710)* adult hermaphrodite. Endosomes were defined as 50 nm or larger membrane-bound structures extending two or more lateral sections. AZ, Active zone. B, Quantification of endosome-like structures in *unc-26(s1710)* adult hermaphrodites.

aptojanin may function in general vesicle trafficking, the process most sensitive to synaptojanin function is vesicle trafficking at the synapse. First, the most obvious defect of *unc-26* animals was their uncoordination; specifically, they exhibited phenotypes typical of defects in synaptic transmission. Second, mutants in general endocytic machinery, such as mutations in the medium subunit of the AP2 complex (Baum, P., and G. Garriga, personal communication), cause severe morphological defects and the mutants have reduced viability. By contrast, *unc-26* mutants were relatively healthy with respect to body shape, brood size, and growth rate. These observations indicated that the phenotypes of *unc-26* mutants are largely attributable to a defect in synaptic function and not general vesicle trafficking.

Our analysis of the *unc-26* mutant revealed defects in multiple steps of synaptic vesicle recycling. Specifically, we observed defects in the recruitment of endocytic machinery, the fission of vesicles from the plasma membrane, the uncoating of vesicles after fission from the membrane, the recovery of vesicles from endosomes, and the tethering of synaptic vesicles to the cytoskeleton in the reserve pool. In contrast to the pleiotropic defects observed at the synapses of *unc-26* mutants, mouse synaptojanin 1 mutants exhibited only an accumulation of coated vesicles at nerve terminals (Cremona et al., 1999). Why do *unc-26* mutants exhibit a larger variety of defects than the mouse mutant? One explanation is that functional redundancy in the mouse rescues some phenotypes. *unc-26* represents the only synaptojanin-like molecule encoded by the *C. elegans* genome, whereas the mouse genome encodes at least one other synaptojanin-like molecule (Khvotchev and Sudhof, 1998). This gene may provide functional redundancy with synaptojanin 1; however, such redundancy can only be partial since synaptojanin 1 mutants are inviable.

How might the known catalytic properties of synaptojanin explain the pleiotropic defects we observed in the synaptic vesicle recycling pathway? Synaptojanin may alter the structural properties of the membrane, or alter the binding properties of the membrane. First, synaptojanin may affect the structural properties of the membrane. During vesicle formation, tight curvature of the membrane at the neck of the bud must be achieved. The phosphatase activity of synaptojanin may facilitate membrane curvature by removing negative charges from the inner membrane surface, thereby relieving the inhibition of lipid-packing caused by repulsion between charged lipids. This model is similar to a mechanism proposed for endophilin, a lysophosphatidic acid acyl transferase. Specifically, endophilin converts inverted cone-shaped lipids to cone-shaped lipids, which favors the negative membrane curvature required for bud formation (Schmidt et al., 1999).

Alternatively, there are a number of proteins implicated in endocytosis that bind polyphosphoinositides. Specifically, synaptotagmin, which is implicated in the recruitment of the clathrin adaptor complex to the plasma membrane (Zhang et al., 1994; Jorgensen et al., 1995), dynamin, which is required for fission of the vesicles (Schmid et al., 1998), and the clathrin adaptor complex, which coats the vesicle (Cremona and De Camilli, 1997), all bind PIs (Schiavo et al., 1996; Zheng et al., 1996; Hao et al., 1997; Jost et al., 1998; Gaidarov and Keen, 1999). Since endocytosis is stalled at each of these steps in the synaptojanin mutant, it is conceivable that cleavage of phosphates from phospholipids is required to release these proteins from the membrane, which allows the next step in the endocytic pathway to proceed.

Finally, the defects we observed in *unc-26* mutants are not consistent with a block at any one of these steps, but are most consistent with an overall kinetic slowing in the synaptic vesicle recycling pathway. Support for this hypothesis is provided first by the variety of defects seen along multiple steps of the pathway, and second, by the continued presence of vesicles, the end product of endocytosis, at synapses. Synaptojanin, therefore, is not essential for synaptic vesicle recycling per se, but more likely accel-

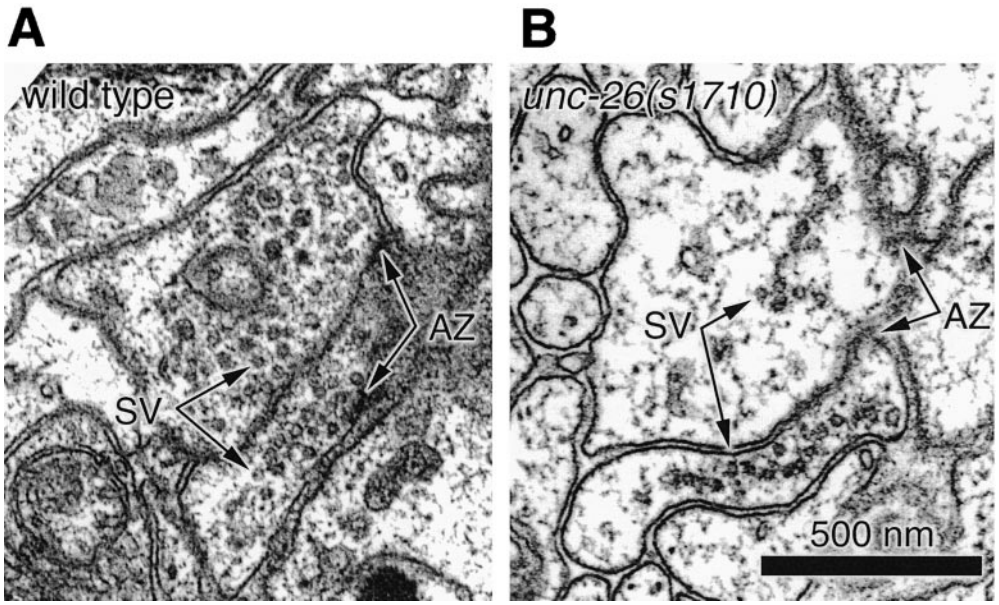

Figure 8. Cytoskeletal defects in an *unc-26* animal. A, Representative micrograph showing typical arrangements of synaptic vesicles in the VD GABA neuron (top) and VA cholinergic neuron (bottom) of a wild-type adult hermaphrodite. AZ, Active zone; SV, synaptic vesicle. B, Representative micrograph showing the linear string of pearls arrangement of synaptic vesicles at synapses in the VD GABA neuron (top) and the VA cholinergic neuron (bottom) of an *unc-26(s1710)* adult hermaphrodite. AZ, Active zone; SV, synaptic vesicle.

erates the progress of intermediates along multiple steps of the synaptic vesicle recycling pathway.

The authors thank Yasuo Nemoto, Pietro De Camilli, Ken Miller, and Jim Rand for sharing results, David Baillie for providing strains, Robert Barstead for providing the cDNA library, Yuji Kohara for providing EST clones, and Alan Coulson for providing cosmids.

T.W. Harris was in part supported by a National Institutes of Health (NIH) Genetics Training Grant Fellowship. H.R. Horvitz is an Investigator of the Howard Hughes Medical Institute. This research was supported by grants from the Huntsman Cancer Institute and NIH grant RO1 NS 34307 to E.M. Jorgensen, and NIH grant GM29663 to H.R. Horvitz.

References

Alfonso, A., K. Grundahl, J.R. McManus, and J.B. Rand. 1994. Cloning and characterization of the choline acetyltransferase structural gene (*cha-1*) from *C. elegans*. *J. Neurosci.* 14:2290–2300.

Bensen, E.S., G. Costaguta, and G.S. Payne. 2000. Synthetic genetic interactions with temperature-sensitive clathrin in *Saccharomyces cerevisiae*. Roles for synaptojanin-like Inp53p and dynamin-related Vps1p in clathrin-dependent protein sorting at the trans-Golgi network. *Genetics*. 154:83–97.

Brenner, S. 1974. The genetics of *Caenorhabditis elegans*. *Genetics*. 77:71–94.

Charest, D.L., D.V. Clark, M.E. Green, and D.L. Baillie. 1990. Genetic and fine structure analysis of *unc-26(IV)* and adjacent regions in *Caenorhabditis elegans*. *Mol. Gen. Genet.* 221:459–465.

Chung, J.K., F. Sekiya, H.S. Kang, C. Lee, J.S. Han, S.R. Kim, Y.S. Bae, A.J. Morris, and S.G. Rhee. 1997. Synaptojanin inhibition of phospholipase D activity by hydrolysis of phosphatidylinositol 4,5-bisphosphate. *J. Biol. Chem*. 272:15980–15985.

Communi, D., and C. Erneux. 1996. Identification of an active site cysteine residue in human type I Ins(1,4,5)P3 5-phosphatase by chemical modification and site-directed mutagenesis. *Biochem. J.* 320:181–186.

Communi, D., R. Lecocq, and C. Erneux. 1996. Arginine 343 and 350 are two active residues involved in substrate binding by human Type I D-myo-inositol 1,4,5,-trisphosphate 5-phosphatase. *J. Biol. Chem*. 271:11676–11683.

Cremona, O., and P. De Camilli. 1997. Synaptic vesicle endocytosis. *Curr. Opin. Neurobiol.* 7:323–330.

Cremona, O., G. Di Paolo, M.R. Wenk, A. Luthi, W.T. Kim, K. Takei, L. Daniell, Y. Nemoto, S.B. Shears, R.A. Flavell, et al. 1999. Essential role of phosphoinositide metabolism in synaptic vesicle recycling. *Cell*. 99:179–188.

David, C., P.S. McPherson, O. Mundigl, and P. De Camilli. 1996. A role of amphiphysin in synaptic vesicle endocytosis suggested by its binding to dynamin in nerve terminals. *Proc. Natl. Acad. Sci. USA*. 93:331–335.

De Camilli, P., and K. Takei. 1996. Molecular mechanisms in synaptic vesicle endocytosis and recycling. *Neuron*. 16:481–486.

De Camilli, P., S.D. Emr, P.S. McPherson, and P. Novick. 1996. Phosphoinositides as regulators in membrane traffic. *Science*. 271:1533–1539.

Fernandez-Chacon, R., and T.C. Sudhof. 1999. Genetics of synaptic vesicle function: toward the complete functional anatomy of an organelle. *Annu. Rev. Physiol.* 61:753–776.

Gaidarov, I., and J.H. Keen. 1999. Phosphoinositide-AP-2 interactions required for targeting to plasma membrane clathrin-coated pits. *J. Cell Biol.* 146:755–764.

Grabs, D., V.I. Slepnev, Z. Songyang, C. David, M. Lynch, L.C. Cantley, and P. De Camilli. 1997. The SH3 domain of amphiphysin binds the proline-rich domain of dynamin at a single site that defines a new SH3 binding consensus sequence. *J. Biol. Chem*. 272:13419–13425.

Guo, S., L.E. Stolz, S.M. Lemrow, and J.D. York. 1999. SAC1-like domains of yeast SAC1, INP52, and INP53 and of human synaptojanin encode polyphosphoinositide phosphatases. *J. Biol. Chem*. 274:12990–12995.

Haffner, C., K. Takei, H. Chen, N. Ringstad, A. Hudson, M.H. Butler, A.E. Salcini, P.P. Di Fiore, and P. De Camilli. 1997. Synaptojanin 1: localization on coated endocytic intermediates in nerve terminals and interaction of its 170 kDa isoform with Eps15. *FEBS Lett.* 419:175–180.

Hao, W., Z. Tan, K. Prasad, K.K. Reddy, J. Chen, G.D. Prestwich, J.R. Falck, S.B. Shears, and E.M. Lafer. 1997. Regulation of AP-3 function by inositides. Identification of phosphatidylinositol 3,4,5-trisphosphate as a potent ligand. *J. Biol. Chem*. 272:6393–6398.

Jefferson, A.B., and P.W. Majerus. 1996. Mutation of the conserved domains of two inositol polyphosphate 5-phosphatases. *Biochemistry*. 35:7890–7894.

Jin, Y., E. Jorgensen, E. Hartwieg, and H.R. Horvitz. 1999. The *Caenorhabditis elegans* gene *unc-25* encodes glutamic acid decarboxylase and is required for synaptic transmission but not synaptic development. *J. Neurosci*. 19:539–548.

Jorgensen, E.M., E. Hartwieg, K. Schuske, M.L. Nonet, Y. Jin, and H.R. Horvitz. 1995. Defective recycling of synaptic vesicles in synaptotagmin mutants of *Caenorhabditis elegans*. *Nature*. 378:196–199.

Jost, M., F. Simpson, J.M. Kavran, M.A. Lemmon, and S.L. Schmid. 1998. Phosphatidylinositol-4,5-bisphosphate is required for endocytic coated vesicle formation. *Curr. Biol.* 8:1399–1402.

Khvotchev, M., and T.C. Sudhof. 1998. Developmentally regulated alternative splicing in a novel synaptojanin. *J. Biol. Chem*. 273:2306–2311.

McIntire, S.L., E. Jorgensen, and H.R. Horvitz. 1993. Genes required for GABA function in *Caenorhabditis elegans*. *Nature*. 364:334–337.

McIntire, S.L., R.J. Reimer, K. Schuske, R.H. Edwards, and E.M. Jorgensen. 1997. Identification and characterization of the vesicular GABA transporter. *Nature*. 389:870–876.

McPherson, P.S., K. Takei, S.L. Schmid, and P. De Camilli. 1994. p145, a major Grb2-binding protein in brain, is co-localized with dynamin in nerve terminals where it undergoes activity-dependent dephosphorylation. *J. Biol. Chem*. 269:30132–30139.

McPherson, P.S., E.P. Garcia, V.I. Slepnev, C. David, X. Zhang, D. Grabs, W.S. Sossin, R. Bauerfeind, Y. Nemoto, and P. De Camilli. 1996. A presynaptic inositol-5-phosphatase. *Nature*. 379:353–357.

Micheva, K.D., B.K. Kay, and P.S. McPherson. 1997. Synaptojanin forms two separate complexes in the nerve terminal. Interactions with endophilin and amphiphysin. *J. Biol. Chem*. 272:27239–27245.

Miller, K.G., A. Alfonso, M. Nguyen, J.A. Crowell, C.D. Johnson, and J.B. Rand. 1996. A genetic selection for *Caenorhabditis elegans* synaptic transmission mutants. *Proc. Natl. Acad. Sci. USA*. 93:12593–12598.

Miller, T.M., and J.E. Heuser. 1984. Endocytosis of synaptic vesicle membrane at the frog neuromuscular junction. *J. Cell Biol.* 98:685–698.

Nguyen, M., A. Alfonso, C.D. Johnson, and J.B. Rand. 1995. *Caenorhabditis elegans* mutants resistant to inhibitors of acetylcholinesterase. *Genetics*. 140: 527–535.

Nonet, M., A.M. Holgado, F. Brewer, C.J. Serpe, B.A. Norbeck, J. Holleran, L. Wei, E. Hartwieg, E.M. Jorgensen, and A. Alfonso. 1999. UNC-11, a *Caenorhabditis elegans* AP180 homologue, regulates the size and protein composition of synaptic vesicles. *Mol. Biol. Cell.* 10:2343–2360.

Nonet, M.L. 1999. Visualization of synaptic specializations in live *C. elegans* with synaptic vesicle protein-GFP fusions. *J. Neurosci. Methods*. 89:33–40.

Olivos-Glander, I.M., P.A. Janne, and R.L. Nussbaum. 1995. The oculocerebrorenal syndrome gene product is a 105-kD protein localized to the Golgi complex. *Am. J. Hum. Genet.* 57:817–823.

Rand, J.B., and R.L. Russell. 1984. Choline acetyltransferase-deficient mutants of the nematode *Caenorhabditis elegans*. *Genetics*. 106:227–248.

Rand, J.B., and R.L. Russell. 1985. Molecular basis of drug-resistance mutations in *C. elegans*. *Psychopharmacol. Bull.* 21:623–630.

Raucher, D., T. Stauffer, W. Chen, K. Shen, S. Guo, J.D. York, M.P. Sheetz, and T. Meyer. 2000. Phosphatidylinositol 4,5-bisphosphate functions as a second messenger that regulates cytoskeleton–plasma membrane adhesion. *Cell*. 100:221–228.

Sakisaka, T., T. Itoh, K. Miura, and T. Takenawa. 1997. Phosphatidylinositol 4,5-bisphosphate phosphatase regulates the rearrangement of actin filaments. *Mol. Cell. Biol.* 17:3841–3849.

Schiavo, G., Q.M. Gu, G.D. Prestwich, T.H. Sollner, and J.E. Rothman. 1996. Calcium-dependent switching of the specificity of phosphoinositide binding to synaptotagmin. *Proc. Natl. Acad. Sci. USA*. 93:13327–13332.

Schmid, S.L., M.A. McNiven, and P. De Camilli. 1998. Dynamin and its partners: a progress report. *Curr. Opin. Cell Biol.* 10:504–512.

Schmidt, A., M. Wolde, C. Thiele, W. Fest, H. Kratzin, A.V. Podtelejnikov, W. Witke, W.B. Huttner, and H.D. Soling. 1999. Endophilin I mediates synaptic vesicle formation by transfer of arachidonate to lysophosphatidic acid. *Nature*. 401:133–141.

Shupliakov, O., P. Low, D. Grabs, H. Gad, H. Chen, C. David, K. Takei, P. De Camilli, and L. Brodin. 1997. Synaptic vesicle endocytosis impaired by disruption of dynamin-SH3 domain interactions. *Science*. 276:259–263.

Simpson, F., N.K. Hussain, B. Qualmann, R.B. Kelly, B.K. Kay, P.S. McPherson, and S.L. Schmid. 1999. SH3-domain-containing proteins function at distinct steps in clathrin-coated vesicle formation. *Nat. Cell Biol.* 1:119–124.

Slepnev, V.I., G.C. Ochoa, M.H. Butler, D. Grabs, and P.D. Camilli. 1998. Role of phosphorylation in regulation of the assembly of endocytic coat complexes. *Science*. 281:821–824.

Stolz, L.E., C.V. Huynh, J. Thorner, and J.D. York. 1998. Identification and characterization of an essential family of inositol polyphosphate 5-phosphatases (INP51, INP52 and INP53 gene products) in the yeast *Saccharomyces cerevisiae. Genetics*. 148:1715–1729.

Suchy, S.F., I.M. Olivos-Glander, and R.L. Nussabaum. 1995. Lowe syndrome, a deficiency of phosphatidylinositol 4,5-bisphosphate 5-phosphatase in the Golgi apparatus. *Hum. Mol. Genet.* 4:2245–2250.

Takei, K., P.S. McPherson, S.L. Schmid, and P. De Camilli. 1995. Tubular membrane invaginations coated by dynamin rings are induced by GTP-gamma S in nerve terminals. *Nature*. 374:186–190.

White, J.G., E. Southgate, J.N. Thomson, and S. Brenner. 1976. The structure of the ventral nerve cord of *Caenorhabditis elegans. Philos. Trans. R Soc. Lond. [Biol.]*. 275:327–348.

Wigge, P., Y. Vallis, and H.T. McMahon. 1997. Inhibition of receptor-mediated endocytosis by the amphiphysin SH3 domain. *Curr. Biol.* 7:554–560.

Woscholski, R., P.M. Finan, E. Radley, N.F. Totty, A.E. Sterling, J.J. Hsuan, M.D. Waterfield, and P.J. Parker. 1997. Synaptojanin is the major constitutively active phosphatidylinositol-3,4,5-trisphosphate 5-phosphatase in rodent brain. *J. Biol. Chem*. 272:9625–9628.

Woscholski, R., P.M. Finan, E. Radley, and P.J. Parker. 1998. Identification and characterisation of a novel splice variant of synaptojanin 1. *FEBS Lett.* 432: 5–8.

Zhang, J.Z., B.A. Davletov, T.C. Sudhof, and R.G. Anderson. 1994. Synaptotagmin I is a high affinity receptor for clathrin AP-2: implications for membrane recycling. *Cell*. 78:751–760.

Zheng, J., S.M. Cahill, M.A. Lemmon, D. Fushman, J. Schlessinger, and D. Cowburn. 1996. Identification of the binding site for acidic phospholipids on the PH domain of dynamin: implications for stimulation of GTPase activity. *J. Mol. Biol.* 255:14–21.